Calibration of the 11-By 11-Foot Transonic Wind Tunnel at the NASA Ames Research Center

Max A. Amaya* and Alan R. Boone†
NASA Ames Research Center, Moffett Field, CA

A series of calibration and flow survey tests were conducted in the 11-By 11-Foot Transonic Wind Tunnel following the modernization of the Unitary Plan Wind Tunnel at the NASA Ames Research Center. These tests included measurements of the static and total pressure which are required to develop the calibration tables used to compute the facility tunnel conditions and to correct the model airplane data for longitudinal buoyancy effects. Measurements of the total temperature, flow angle, and boundary layer characteristics were also made to provide an indication of the flow quality in the test section. Calibration parameters were determined for both test section wall configurations; slots normal for full-span model testing and floor slots sealed for semi-span model testing.

Nomenclature

Cp = pressure coefficient
Cp_m = pressure coefficient, measured
Cp_{fit} = pressure coefficient, derived from a curve-fit
$C_{PS,cor}$ = static pressure coefficient correction
$C_{PT,cor}$ = total pressure coefficient correction
K_ϕ = five-hole cone probe rotation factor
$K_{\alpha 1}$ = 5-hole cone probe pitch sensitivity determined from calibration
$K_{\alpha 2}$ = 5-hole cone probe pitch offset determined from calibration
$K_{\beta 1}$ = 5-hole cone probe yaw sensitivity determined from calibration
$K_{\beta 2}$ = 5-hole cone probe yaw offset determined from calibration
$K_{T,rec}$ = probe total temperature recovery factor
M = Mach number computed from $P_{S,ts}$ and $P_{T,ts}$
M_c = Mach number computed from $P_{S,pc}$ and $P_{T,sc}$
$P1, P3$ = pitch sensing taps on the 5-hole cone probe
$P2, P4$ = yaw sensing taps on the five-hole cone probe
$P_{S,pc}$ = static pressure measured in the test section plenum chamber
$P_{S,pipe}$ = static pressure measured by the static pipe
$P_{S,ts}$ = corrected test section static pressure at the model reference location
$P_{S,probe}$ = static pressure on the five-hole cone probe used for reference
$P_{T,sc}$ = total pressure measured in settling chamber
$P_{T,probe}$ = total pressure measured by the five hole cone probe
$P_{T,ts}$ = corrected test section total pressure at the model test section reference location
q_c = dynamic pressure computed from $P_{S,\mathrm{pc}}$ and M_c
q_{probe} = dynamic pressure computed from $P_{S,\mathrm{probe}}$ and $M_{,\mathrm{probe}}$
$T_{T,probe}$ = probe total temperature measured during Flow Uniformity Survey
$T_{T,Pcor}$ = corrected probe total temperature measured during Flow Uniformity Survey
$T_{T,F}$ = tunnel total temperature measured upstream of contraction, degrees Fahrenheit
T_T = tunnel total temperature, degrees Rankine
u_e = velocity at the boundary layer edge
u_L = local velocity in the boundary layer

* Aero Engineer, Wind Tunnel Operations Branch, AIAA Member
† Aero Engineer, Wind Tunnel Operations Branch, AIAA Senior Member

x, y, z = streamwise, spanwise & vertical coordinates; zero at the centerline of the flow passage; z is positive for top; y is positive for south; x=0 is defined at the start of the test section and is positive downstream

α_{SA} = A-plane stream angle in the tunnel coordinate system
α_m = pitch flow angularity in the probe coordinate system
α_{Probe} = probe pitch angle in the tunnel coordinate system
β_{SA} = B-plane stream angle in the tunnel coordinate system
β_m = yaw flow angularity in the probe coordinate system
β_{Probe} = probe yaw angle in the tunnel coordinate system
δ = boundary layer thickness where $V_L = 0.99$ of V_e
δ_1 = boundary layer displacement thickness
δ_2 = boundary layer momentum thickness
ϕ = 5-hole cone probe roll orientation angle
ρ_e = density at the boundary layer edge
ρ_L = local density in the boundary layer

Acronyms:
AIAA = American Institute of Aeronautics and Astronautics
A/D = Analog to Digital
DTC = Digital Temperature Compensation
ESP = Electronically Scanned Pressure
FSP = Functional Subsystem Processor
MUA = Make-Up Air compressor
NIST = National Institute of Standards and Technology
PES = Plenum Evacuation System
PPM = parts per million
PSI = Pressure Systems, Inc.
PWT = Pressure Wind Tunnel
RTD = Resistance Temperature Detector
SDS = Standard Data System
SMP = Subsystem Management Processor
SMSS = Sting Model Support System
TMSS = Turntable Model Support System
TRS = Turbulence Reduction System consisting of honeycomb and two screens
TS = Tunnel Station; TS 0 defined at the start of the test section; Same as x; inches
TWT = Transonic Wind Tunnel
UPWT = Unitary Plan Wind Tunnel

I. Introduction

THE comprehensive calibration and flow quality surveys of the 11-By 11-Foot Transonic Wind Tunnel (TWT) include a static pipe calibration, a flow uniformity survey, a turbulence and acoustics survey, and an LB-435 calibration model test.

The static pipe calibration test measures the static pressure distribution through the nozzle and test section. The pipe consists of 444 static pressure taps distributed along the 60-ft pipe length at various spacing intervals. Static pressure calibration tables are generated for full-span and semi-span test section configurations, and data are used to generate clear tunnel buoyancy corrections.

The flow uniformity survey measures the uniformity of the total pressure, flow angularity, and temperature as well as boundary layer characteristics for full-span and semi-span test section configurations. Data are used to create total pressure correction tables. Five-hole cone probe results are useful for evaluating flow anomalies in the test section and flow-angularity characteristics for semi-span models. For full-span models, flow angle corrections to the data are generally determined by testing models in the upright and inverted attitudes.

The turbulence and acoustics survey measures the three components of the nondimensional fluctuating mass-flux or "turbulence level" using hot-wire anemometry and noise or "acoustic level" using differential dynamic pressure transducers. Turbulence levels can be an important factor in testing laminar flow airfoils where high levels of free-stream turbulence can cause premature transition of the airfoil boundary layer. Acoustic measurements are used to support weapons bay testing by providing background noise measurements for the test section.

The LB–435 calibration model test measures the integrated effects of test section flow quality on an actual transport airplane model, tracks flow angularity, and evaluates data repeatability along with test techniques and processes. This model has been tested many times in the 11-By 11-Foot TWT.

The present paper discusses the static pipe calibration and flow uniformity survey following the modernization of the 11-By 11-Foot TWT.[1,2] The primary goal of these two tests was to prepare calibration tables for the 11-By 11-Foot TWT which provide the relationship between the facility's institutional total and static pressure measurement and the total and static pressure measurement at the reference point of the model. These tables supply the information that allows the computation of the test Mach number, dynamic pressure, and model buoyancy for the particular mounting location of a test article in the test section.

Data for the static pipe calibration and flow uniformity survey are acquired for both full-span and semi-span test section configurations. For the full-span configuration, all the test section baffled wall slots are open, allowing air exchange between the test section and the plenum. For the semi-span configuration, the floor baffles are removed and replaced with solid fillers to provide a solid reflection plane.

II. Facility description

The Unitary Plan Wind Tunnel (UPWT) consists of three tunnel legs: the 11-By 11-Foot TWT, the 9- by 7-Foot Supersonic Wind Tunnel, and the 8- by 7-Foot Supersonic Wind Tunnel (Fig. 1). The two supersonic legs share a common 11-stage axial-flow compressor and aftercooler drive leg, and they use diversion valves at the ends of a common drive leg. A three-stage axial-flow compressor drives the 11-By 11-Foot TWT. A common drive motor system can be coupled to either the 3-stage or 11-stage compressor. One tunnel can therefore be run while test articles are being installed in or removed from the other two.

The 11-By 11-Foot TWT leg is a closed-circuit, variable-pressure, continuous operation wind tunnel (Fig. 2). Subsonic Mach number control involves setting the compressor drive speed to one of ten setpoints and using variable-camber inlet guide vanes for fine Mach number control. Supersonic Mach number control involves setting the flexible wall nozzle to achieve the proper area ratio in addition to setting the compressor drive speed and the inlet guide vanes. A tandem diffuser system with an annular diffuser followed by a wide-angle diffuser is upstream of a 70-ft-diameter aftercooler section in the drive leg. Flow-smoothing vanes are located in the tandem diffuser to improve flow uniformity entering the heat exchanger and temperature uniformity in the test section. The settling chamber upstream of the contraction is 38 feet in diameter. A Turbulence Reduction System (TRS) located in the settling chamber includes a 1-in.-cell-diameter, 20-in. long honeycomb for flow straightening followed by two 0.041-in.-diameter-wire, 6-mesh screens for turbulence reduction. The contraction provides a transition from the circular cross section of the settling chamber to the square cross section of the test section. The contraction ratio is 9.4. The test section is 11-By 11-feet in cross section and 22 feet in length. Slots in all four walls run the full length of the test section. The slots contain baffles that provide a 6-percent porosity into the plenum chamber. Ejector flaps on all four walls at the exit of the test section can be set remotely to control the plenum flow bypassed from the test section. Flow exits the test section and enters a transition region back to the circular main diffuser. A Plenum Evacuation System (PES) provides an active method of removing air from the test section plenum by using the Make-Up Air compressor system (MUA) of the auxiliaries facility.

III. Tunnel conditions, hardware, and instrumentation

A. Static and total pressure

The tunnel plenum static pressure $P_{S,pc}$ is sampled from eight tubes located within the plenum chamber surrounding the test section. The tube bundle is located streamwise at Tunnel Station (TS) 30, laterally at y = 118 in. (52 in. outward from the test section wall), and vertically at z = 0 in. (the tunnel centerline). Two of the tubes supply the primary and backup $P_{S,pc}$ measurement used to compute Mach number in the data system. The tubes are connected to pressure transducers located in racks that are within a foot in elevation of the tunnel centerline.

The uncorrected tunnel total pressure $P_{T,sc}$ is sampled from three identical rakes located in the settling chamber just downstream of the turbulence reduction screens. Each rake has eight pitot probes, and each probe is manifolded to its counterpart on the other rakes and pneumatically connected and routed out of the tunnel. Two of these sources serve as the primary and backup $P_{T,sc}$ measurements used to determine Mach number in the data system. The probes are connected to pressure transducers located in racks that are within a foot in elevation of the tunnel centerline. The additional $P_{S,pc}$ and $P_{T,sc}$ source probes are also routed out of the tunnel and are used as sources for the facility's control system (FCS) measurements, as redundant sources for the data system, or as auxiliary sources for testing purposes (i.e., as test-dependent reference pressures or calibration pressures).

The $P_{S,pc}$ and $P_{T,sc}$ pressures used to determine the test section Mach number are measured with the facility's Flow Reference System (FRS). Two complete Flow Reference Systems are used for all tests, a primary and a backup. Each system comprises four precision transducers with different sensing ranges. Two quartz transducers sense $P_{T,sc}$ and two special high-accuracy silicon transducers sense the pressure differential $P_{T,sc} - P_{S,pc}$. The absolute transducers sensing $P_{T,sc}$ have ranges of 15 and 45 psia and accuracy ratings of 0.01 percent of full scale. The transducers sensing the differential pressure $P_{T,sc} - P_{S,pc}$ have ranges of 10 and 30 psid and accuracy ratings of 0.02 percent of full scale. The transducers are calibrated on a fixed schedule against NIST traceable standards. Built-in overpressurization features protect the low-range transducers from damage. Depending on the facility operating speed and pressure, software selects between the low or high range $P_{T,sc}$ and $P_{T,sc} - P_{S,pc}$ measurements to give the best Mach number accuracy. Uncertainty analysis of this system has determined that Mach number errors caused by flow reference system measuring errors are less than ±0.0005 for all operating conditions within the facility test envelope.

B. Tunnel total temperature

The tunnel total temperature $T_{T,F}$ is measured using four Resistance Temperature Detector (RTD) probes. The probes are located on the corner vanes upstream of the settling chamber and distributed on the face of the turning vanes in the core flow. The four temperature readings are averaged to obtain a temperature measurement representative of the flow cross section. The accuracy of these temperature probes is stated by the manufacturer to be ±2.0 °F.

C. Specific humidity

A microprocessor-controlled humidity analyzer is used to measure the moisture content of the air within the tunnel circuit. The analyzer uses a chilled-mirror dew-point sensor and a pressure transducer to determine dew-point temperature, absolute pressure, and other psychometric variables. Data from a primary and backup analyzer are recorded to the data system in units of parts per million (ppm) by weight. The accuracy of the humidity measurement is ±50 ppm by weight.

The humidity measurements are used as indicators of when to increase the dry air exchange rate or, in some cases, when to cease testing to purge the humid tunnel air and replenish with dry air. For most tests, a maximum limit of 500 ppm by weight is used to guide dry air exchange and purge decisions. Wind tunnel flow condition data are not corrected for tunnel humidity effects in the data system.

IV. Calibration goals

The primary goal of the static pipe calibration test was to determine the test section static pressure calibration tables for full-span and semi-span test section configurations, as well as to:

- Determine the in-test data repeatability of the calibration factors.
- Establish time histories of institutional tunnel condition pressures at several selected Mach numbers.
- Determine the amplitude and frequency content (0.1 Hz < frequency < 10 Hz) of the $P_{S,pc}$ and $P_{T,sc}$ variation for its effect on test data accuracy.
- Determine a time correlation between pipe pressures and $P_{S,pc}$ to ascertain the effect of pneumatic tube lag and damping on calibration accuracy.

For the flow uniformity survey, the primary goal was to determine the test section total pressure calibration tables for full-span and semi-span test section configurations as well as to:

- Map the total pressure, total temperature, and flow-angle uniformity in the survey regions.
- Measure the boundary layer profiles at three test section streamwise locations, and determine the displacement thickness and momentum thickness.

V. Calibration equipment

A. Static pipe installation

The test installation of the static pipe is shown in Fig. 3. For this calibration, the 6-in. diameter static pipe was mounted at two heights within the test section. The centerline height was used to determine calibration data for full-span model tests, whereas the position 33 in. below centerline was used to determine the tunnel calibration data for semi-span model tests.

The pipe was suspended between a set of tensioning cables at the upstream end and the Sting Model Support System (SMSS) at the downstream end. A hydraulic cylinder connected the static pipe to the SMSS through clevis/pin joints. The cylinder provided up to 10,000-lbf tension to add stiffness and stability to the pipe.

The pipe is composed of five 10.25-ft long segments that are connected end-to-end with Marmon clamps. The clamps were hand fitted to provide an extremely smooth connection between pipe sections. The pipe sections were numbered one through five starting at the downstream end and progressing upstream. The first two pipe segments were instrumented with pressure taps at 3-in. intervals longitudinally along the pipe. At each axial station, four pressure taps were placed 90° from one another. In addition, each set of four taps was rotated about the pipe centerline by 15° from its upstream neighbors so that the downstream taps were not within the disturbance flow field of the upstream taps. Pipe 3 had pressure taps at 6-in. intervals, pipe 4 at 12-in. intervals, and pipe 5 was not instrumented. There were a total of 444 separate pressure taps on the four instrumented pipe segments. The first two segments extended through the length of the slotted test section and contained 324 of these taps.

B. Static pipe instrumentation

Miniature Electronically Scanned Pressure (ESP) instrumentation with Digital Temperature Compensation (DTC) was used to measure the pressures associated with the calibration test ($P_{S,pipe}$) along the static pipe. With DTC, each of the pressure sensors in the ESP module is characterized for temperature dependence within the instrumentation firmware. As pressure data are acquired during tests, the temperature of each individual transducer is sensed and corrections are applied to the measurements to account for temperature-induced drift. This feature gives the system a remarkable degree of stability and accuracy and reduces the overall calibration requirements.

A stable monitor pressure was measured on each DTC ESP module, as well as on a high-accuracy quartz transducer. The pressure measuring accuracy, as indicated by the monitor pressure error, remained well within the manufacturer's specification for many hours of continuous testing. The largest single source of instrument error on previous calibrations using the older technology ESP units had been temperature drift on the transducers, which occurred at different rates and in opposite directions.

Modules populated with 5-psid transducers were used for most of the static pipe pressures that were located within the test section. Pressures extending into the nozzle section were measured with 15-psid transducers. Referring to Fig. 3, pressures upstream of TS –48 and downstream of TS 232 were measured with two 15-psid instruments, and all others were measured with six 5-psid units. The manufacturer's specification for accuracy on the transducers was 0.05 percent of the transducer's full scale rating. This translates to ±0.36 psf for the 5-psid modules and ±1.08 psf for the 15-psid units.

An uncertainty analysis undertaken during the test planning period revealed that the key to calibration accuracy was accurately measuring the pressure difference ($P_{S,pipe} - P_{S,pc}$). With this in mind, seven unused ports on each of the static pipe modules were pneumatically connected to the extra facility $P_{S,pc}$ pressure. The data were then reduced in a manner that removed the error associated with the module reference pressure transducer (so that it was not included in the overall error budget) by making it a "common mode," or "correlated," biasing error. The overall instrumentation uncertainty for measuring the pressure difference ($P_{S,pipe} - P_{S,pc}$) was nominally ±0.23 psf for the 5-psid modules and ±0.56 psf for the 15-psid units.

C. Flow uniformity installation

Models mounted on the SMSS are generally positioned to locate the balance center in the range from TS 155 to TS 165. Semi-span models are mounted on the turntable model support system (TMSS), which is situated on the floor at TS 106. The flow uniformity test surveyed the flow field near TS 165 and 106 using two hardware installations. A flow-angle probe and a total temperature probe were used to make local measurements of total pressure, flow angularity, and total temperature. In addition, boundary layer rakes were positioned at three streamwise locations to measure the boundary layer growth characteristics in the test section.

A planar survey at TS 165 was conducted using the MK XII traversing head survey apparatus, shown in Fig. 4. The MK XII consists of a 0°-sweep, 80.5-in. span, symmetric wing with a traversing head (mouse). The mouse supports both the flow angle and the total temperature probes and has a cavity for instrumentation. The temperature

probe was mounted 2.5-in. above the flow-angle probe. The mouse, which was remotely controlled, was traversed laterally across the wing over a $y = \pm 30$ in. range. The entire apparatus was supported by sting hardware mounted to the SMSS, allowing vertical translation of $z = \pm 36$ in. Stress load limitations prevented the MK XII from being used at supersonic conditions, so it was replaced with a probe holder. This fixed the flow-angle probe position on the tunnel centerline ($y = 0$ in.) and the temperature probe at $y = 3.5$ in.

The same probe holder was used for a centerline survey at TS 106 over a vertical range of $z = -54$ to 24 in. For this measurement, the floor slot baffles were removed and replaced with solid fillers to provide the reflection plane necessary for semi-span model testing.

D. Flow uniformity instrumentation

Flow-angularity and total pressure data were collected from a five-hole cone probe with holes arranged on a 40° conical nose and a set of static-sensing taps arranged on the aft body (Fig. 5). Pressure differences across the cone were measured using temperature-compensated, 1-psid pressure transducers. The manufacturer-quoted accuracies are 0.06 percent "best straight line" with ±0.025 percent of full scale per °F for thermal zero shift and ±0.01 percent of reading per °F for thermal sensitivity shift. The transducers were calibrated at the NASA Ames Metrology lab using equipment traceable to NIST standards. The probe total and static pressures were each plumbed to eight ports on a 15-psid, DTC ESP module.

Probe angle of attack was measured using a precision accelerometer. The accelerometer was placed in the traversing head for the MK XII installation and in the instrumentation cavity on the supersonic probe holder. Accelerometers were calibrated at the NASA Ames Metrology lab and re-zeroed in the test section against a standard with an accuracy of 0.005°. Probe sideslip angle was measured using the SMSS knuckle-sleeve device, which uses a pair of rotating bent arms called the knuckle and the sleeve to obtain taper angles in the pitch and yaw planes anywhere between ±15°. The angular offsets between the probe tip and the angle measurement devices were carefully measured and accounted for in the data reduction. The horizontal position of the probe along the y-axis was measured using an encoder, and the vertical position along the z-axis were measured using a string pot.

Test section total temperature $T_{T,\text{probe}}$ was measured with an RTD mounted in a shielded probe holder. The accuracy of this airflow probe was stated by the manufacturer to be ±2.0 °F.

Boundary layer characteristics were defined from measurements using three 10-in.-high rakes. Each rake was instrumented with twenty 0.04-in.-diameter pitot probes. The probes were plumbed to 15-psid transducers on DTC ESP modules. The boundary layer rakes were positioned on the test section floor with rake 1 at $x = 36$ in., $y = 0$ in.; rake 2 at $x = 106$ in., $y = 10.4$ in.; and rake 3 at $x = 176$ in., $y = -10.4$ in.

Redundant facility $P_{T,sc}$ and $P_{S,pc}$ pressures were measured using eight ports on the same DTC ESP modules used for the flow-angle probe pressures. As with the static pipe, these pressures were used in the data reduction to minimize the bias error associated with the ESP module reference pressure.

VI. Data acquisition

Steady-state data were acquired using the wind tunnel facility's Standard Data System (SDS). The SDS consists of a Subsystem Management Processor (SMP), a number of Functional Subsystem Processors (FSPs), and a large number of X-terminals that provide wind tunnel personnel with graphical user interfaces to the features of SDS. The SMP is an Enterprise 3500 server (Sun Microsystems, Santa Clara, CA) running the Solaris operating system. The SMP manages the overall data acquisition activity in a facility. Its tasks include coordinating the FSPs, interfacing with the automated tunnel condition and model attitude control systems, and providing a command and control interface for operations personnel. The SMP also provides visualization and analysis tools for both the real-time and near-time data streams. FSPs are Pentium-class PCs running LynxOS Real-Time UNIX (Lynx Real-Time Systems, Inc.). These modular units are responsible for collecting data from particular types of sensors. The six FSP instrument categories are balance, surface pressure, digital, general purpose analog, tunnel condition/model attitude, and temperature. Each FSP was designed to perform instrument-specific data acquisition tasks for collecting the highest quality data at the sensor and instrument's maximum throughput. Sensor data are transmitted in parallel across a 100 Base-T Ethernet highway to the SMP, where they are averaged, converted to common engineering units, and further reduced to test-specific final results.

A. Static pipe data acquisition

The static pipe test provided one set of calibration tables for sting-mounted models and a second set for turntable-mounted semi-span models. The calibration tables for semi-span testing were measured with the static pipe located 33 in. below the tunnel centerline, which more closely matches the model reference point of semi-span models. Data were normally recorded in groups of six data points with a 30-sec delay programmed between data points. Several of the calibration test conditions were repeated up to five times over the duration of the test so that repeatability statistics could be extracted from the test database. All data were acquired using a one second sampling period, which was determined to be optimum during an initial sampling study. The reference pressure used for the static pipe ESP modules was a steady "driven" or controlled pressure and was set to be within ±0.5 psi of the tunnel static pressure as the tunnel was set to the desired Mach number and total pressure. Pressures were allowed to settle for several minutes before data were taken at the new tunnel conditions.

B. Flow uniformity data acquisition

Test section flow properties were measured at Mach numbers of 0.4, 0.6, 0.8, 0.85, 1.2, and 1.4 and at total pressures of 2120, 3180, and 4600 psf. A sampling study was initially performed, and a one second duration was chosen for data acquisition. A flow-angle probe calibration was performed at 3180 psf for subsonic Mach numbers and at 2120 psf for supersonic Mach numbers with the flow-angle probe on the centerline at TS 165. The calibration involved pitching the probe from –2° to 2° in 0.25° increments for four probe orientations, ϕ = 0°, 180°, 90°, and 270°. The MK XII survey apparatus was then installed, and the planar survey was conducted at TS 165. The mouse was traversed horizontally from y = –30 to 30 in., in 6-in. increments. At each horizontal position, the survey apparatus was traversed from z = –36 to 36 in., in 6-in. increments. After the survey was completed for a given tunnel conditions set point, the next calibration condition was set and the probe positioning was conducted in the reverse order. For the supersonic test conditions, the MK XII was replaced with the probe holder and a centerline survey was conducted from z = –36 to 36 in., in 6-in. increments.

For evaluating the flow uniformity for the semi-span model test, the centerline survey hardware was moved to TS 106 and the slot baffles were removed from the test section floor and replaced with solid fillers. The centerline survey was conducted from z = –54 to 24 in., in 6-in. increments. Boundary layer rakes were initially installed in the test section for the survey at TS 165 but were removed when they interfered with the flow-angle measurements at the supersonic conditions.

VII. Data reduction

A. Calibration equations

The static pipe and flow uniformity tests provide the calibration tables to correct the facility's institutional total and static pressure measurement to the true total and static pressure in the test section. The tables provide one correction factor for static pressure, $C_{PS,\mathrm{cor}}$, and a second factor for total pressure, $C_{PT,\mathrm{cor}}$. These factors are defined as follows:

$$C_{PS,cor} = \left(\frac{P_{S,pipe} - P_{S,pc}}{q_c} \right) \tag{1}$$

and

$$C_{PT,cor} = \left(\frac{P_{T,probe} - P_{T,sc}}{q_C} \right) \tag{2}$$

Each of the calibration tables contains entries for 38 test section locations at 3-in. intervals, 15 Mach numbers, and 4 total pressures. When a data reduction program is set up for a test project, the streamwise location of the model reference point in the test section and the test type (full-span or semi-span) are specified. A lookup table is then extracted from the calibration table, which includes correction factors at the 15 calibrated Mach numbers and 4 calibrated total pressures. During the test project, this table was used to obtain correction factors for $P_{T,sc}$ and $P_{S,pc}$. For intermediate points between the calibrated test conditions, linear interpolation was performed on both $P_{T,sc}$ and M_c to arrive at the proper correction factors. Linear extrapolation was used to determine the correction factors for points outside the calibrated test conditions.

The correction factors were used to generate corrected test conditions as follows:

$$P_{S,ts} = P_{S,pc} + C_{PS,cor} \times q_c \tag{3}$$

and

$$P_{T,ts} = P_{T,sc} + C_{PT,cor} \times q_c \tag{4}$$

The calibrated tunnel Mach number and dynamic pressure were then computed from $P_{S,ts}$ and $P_{T,ts}$ using standard compressible flow equations (Reference 4).

B. Flow uniformity equations

1. Local A*-plane and* B*-plane flow angles*

Flow angularity in the 11-By 11-Foot TWT is referenced to the tunnel coordinate system whose origin is located at the start of the test section along the centerline (Fig. 4). The flow angle α is in the *A*-plane, which is the vertical plane defined by the *x–z* axis. The flow angle β is in the *B*-plane, which is the horizontal plane defined by the *x–y* axis. The sign conventions for flow angularity are defined in Fig. 5. Positive α is flow coming up from the floor, positive β is flow from the south wall to the north wall, or from the right to the left, pilots view.

The local flow angles in the *A*-plane and *B*-plane were defined by

$$\alpha_m = \left[K_{\alpha 1} \times \left(\frac{P3 - P1}{q_{probe}} \right) + K_{\alpha 2} \right] \times K_{\phi} \tag{5}$$

and

$$\beta_m = \left[K_{\beta 1} \times \left(\frac{P4 - P2}{q_{probe}} \right) + K_{\beta 2} \right] \times K_{\phi} \tag{6}$$

The local flow angularity was then adjusted for the probe angle of attack and sideslip to give the flow-angularity properties in the tunnel coordinate system.

$$\alpha = \alpha_m - \alpha_{probe} \tag{7}$$

and

$$\beta = \beta_m - \beta_{probe} \tag{8}$$

2. Total temperature

Test section total temperature variation is an important indicator of transonic test section flow quality. A temperature recovery factor was computed to evaluate the probe performance,

$$K_{T,rec} = \left(\frac{T_{T,probe} - T_S}{T_T - T_S} \right) \tag{9}$$

The probe temperature was then corrected using the recovery factor,

$$T_{T,Pcor} = T_{T,probe}\left[\frac{1+0.2\times M^2}{1+0.2\times K_{T,rec}\times M^2}\right] \tag{10}$$

3. Boundary layer

The boundary layer displacement thickness and momentum thickness were computed from the rake total pressures and the free-stream tunnel conditions using the following equations:

Displacement thickness

$$\delta_1 = \int_0^{\delta}\left(1-\frac{\rho_L V_L}{\rho_e V_e}\right)dy \tag{11}$$

Momentum thickness

$$\delta_2 = \int_0^{\delta}\left(\frac{\rho_L V_L}{\rho_e V_e}\left(1-\frac{V_L}{V_e}\right)\right)dy \tag{12}$$

The pressure data, the standard definition for Mach number, and a temperature profile that assumed an adiabatic wall boundary condition were used to determine the ratios of the local velocity to the edge velocity and the local density to the edge density.

Ratio of the local velocity to that at the boundary layer edge

$$\frac{u_L}{u_e} = \left(\frac{M_L}{M_e}\right)\times\sqrt{\frac{1.0+0.2\times K_{T,rec}\times\left(M_e\right)^2}{1.0+0.2\times K_{T,rec}\times\left(M_L\right)^2}} \tag{13}$$

where $K_{T,rec}$ is the temperature recovery factor (0.986).

Ratio of the local density to that at the boundary layer edge

$$\frac{\rho_L}{\rho_e} = \left(\frac{T_e}{T_L}\right) = \left(\frac{1.0+0.2\times K_{T,rec}\times\left(M_L\right)^2}{1.0+0.2\times K_{T,rec}\times\left(M_e\right)^2}\right) \tag{14}$$

C. Data reduction methods for the static pipe

At any given axial position along the static pipe, the four measured pressures were averaged and converted to pressure coefficient form using Eq. (1). The plotted symbols in Fig. 6 are the average of all of the data points that were acquired during the test period for the given test condition (Mach 0.95, $P_{T,sc}$ = 2125 psf). For this particular test

condition, each symbol is an average of 120 data points. The heavy solid line in Fig. 6 is a plot of a smoothing curve fit determined from the set of averaged data. A polynomial curve fit method was used for all calibration data from Mach 0.2 through 1.0. For supersonic test conditions, a "boxcar" smoothing algorithm was used because the pressure distributions did not fit the polynomial pattern. Weak tunnel- and static-pipe-generated shocks and expansions caused the more erratic pressure distributions that were measured at supersonic conditions. Curve fit results were used to generate both the tunnel control system tables for setting tunnel Mach number and Reynolds number and data-reduction system tables for computing Mach numbers and Reynolds numbers for test projects.

D. Data reduction methods for flow uniformity

Established procedures were used for calibrating the five-hole cone probe in the test section for various Mach numbers at a tunnel total pressure of 3180 psf. These procedures involved pitching the probe at four roll orientations, $\phi = 0°$, 180°, 90°, and 270°. Calibration constants derived from calibration runs were applied to the measured pressure data to compute the local flow-angularity properties of the tunnel using Eq. (5) to (8). Data were then processed using commercially available data analysis software to produce flow-angle vector plots. An average recovery factor of 0.94 was determined from the temperature data and used to compute the corrected temperature in the test section for all runs.

VIII. Calibration results

A. Factors affecting the static pipe calibration results

1. Temporal variation of test section flow

The standard deviations of the pipe *Cp*'s at Mach 0.95 and $P_{T,sc}$ = 2125 psf are presented in Fig. 7. The data points were recorded once per second for 120 sec. The odd shape shown in Fig. 7 with its minimum point near TS 230 and continuously varying standard deviation is caused by a combination of pneumatic lag in the pressure tubing of the pipe and a low-frequency, small-amplitude time variation of test section static pressure. The pressure-scanning modules were mounted in the instrumentation enclosure of the SMSS. The pressure tubing from the module to the port, therefore, increased in length from the ports at the downstream end of the pipe to the upstream end.

A comparison of the time variation of the facility reference static pressure $P_{S,pc}$ and the measured static pipe pressure at TS 230 (the standard deviation minimum point in Fig. 7) is presented in Fig. 8. The normalized deviations of the two pressures are compared so that time correlation is clearly illustrated within a single figure. Both the phasing and standard deviation of the time variation of these two pressures are nearly identical. The correlation coefficient of the two pressures is indicated on the figure as 0.997. At this location on the static pipe, the pneumatic damping characteristic of the tubing is equal to the damping of the $P_{S,pc}$ pressure tubing. At TS 110, the pressure tubing connecting the static pipe port to the pressure scanning module is 120 in. longer than it is for the taps at TS 230. The comparison of the normalized deviation of the pipe pressure at this location is shown in Fig. 9. This figure shows that the pipe pressure at TS 110 is lagging in time and has a reduced standard deviation with respect to the $P_{S,pc}$ pressure. At TS 0, the pressure tubing connecting the static pipe port to the pressure scanning module is 230 inches longer than it is for the taps at TS 230. Figure 10 shows that this pipe pressure lags more and shows a further reduced standard deviation with respect to $P_{S,pc}$. The effect of the combination of the tunnel time varying flow and the pneumatic tubing damping/lag differences results in added precision uncertainty averaging about ±0.001 to the measured static pipe pressure coefficients. Smoothing by curve fit and averaging of multiple data points negates most of the effects of this source of data inaccuracy.

2. Effects of test section slots

Curve fits for the semi-span calibration for Mach 0.6 to 1.0 are shown in Fig. 11. The negative pressure gradient at the start of the test section is attributed to the relieving effects of the test section slots, which start at TS 0.

3. Mounting interference effects

Referring again to Fig. 11, the positive pressure gradient near the downstream end of the test section is believed to be caused by interference effects from the static pipe hydraulic cylinder fairing and the 11-By 11-Foot TWT SMSS, which feed forward into the test section. Since the shape and volume of the static pipe fairing is similar to the stings and adapters commonly used to support sting-mounted models, no additional Mach corrections are currently

used to account for this mounting interference. This pressure distribution is used to compute a clear tunnel buoyancy correction that is applied to the measured model forces.

4. Tap error and pipe joint effects

The curve fit residuals ($Cp_m - Cp_{fit}$) for the Mach range from 0.6 to 1.0 are shown in Fig. 12. The residuals are caused by tap error in the pipe pressure measurements. Tap error is a result of local imperfections at the tap or on the pipe surface in the neighborhood of the tap. It can be seen in Fig. 12 that the curve fit residuals are nearly identical for this range of test section Mach number, which infers that the residuals are an artifact of the pipe or pipe taps rather than of the flow in the tunnel. The static pipe is also used to calibrate the 12-Foot Pressure Wind Tunnel. Results from the 12-Foot Pressure Wind Tunnel facility calibration were compared with those seen in Fig. 12 and showed remarkably similar residuals. This suggests that tap error is the cause of the small-scale variation in measured pressure along the test section length and that it justifies the smoothing procedure used in the calibration data reduction. The large residuals shown near TS 5 and 125 coincide with the joints in the static pipe assembly between adjacent 10.25-ft pipe sections (see Fig. 3).

5. Instrumentation error effects

During the planning phases of the static pipe calibration, uncertainty analysis was used to guide choices of instrumentation, instrumentation hookup, and data-reduction procedures. Figure 13 shows the results of these uncertainty analyses for the actual instrumentation, instrument hookup, and data reduction program that was used. The goal for the calibration was to limit the Mach errors due to the instrument error sources to ±0.001 for all test conditions within the test matrix. On the basis of the data checking and repeat data points that were recorded during the calibration, the instrumentation performed to the specifications claimed by the manufacturers.

B. Calibration results for the static pipe

1. Mach number effects

The effect of Mach variation on the test section *Cp* for subsonic and supersonic operation can be seen in Fig. 14 and Fig. 15, respectively. Within these figures, the Mach number is varied while the facility total pressure is maintained at 2125 psf. The most noticeable trends shown in Fig. 14 are the increase in the slot effect for increasing Mach number at TS 0 and the decrease in the "forward feeding" interference effect of the static pipe fairing and the sting model support for increasing Mach numbers. For supersonic Mach numbers (Fig. 15), the obvious change is a greater longitudinal variation of the *Cp* in comparison to subsonic values, especially in the forward half of the test section. These effects are attributable to the discontinuity in the wall boundary condition where the test section slots begin. Small mass additions through the slots produce diffuse tunnel shocks that originate in the first foot of the test section. A second obvious difference between the subsonic and supersonic *Cp* distributions is the absence of a pressure influence from the pipe hydraulic cylinder fairing and the SMSS at the downstream end of the static pipe. The supersonic test section flow effectively eliminates upstream propagation of the pressure disturbance arising from the fairing and support system.

2. Reynolds number effects

Subsonic and supersonic Reynolds number effects on the test section *Cp* distribution are summarized in Fig. 16 and Fig. 17, respectively. The Mach number is fixed for the data contained within the figures, whereas the tunnel total pressure is varied through the setpoint values of 0.5, 1.0, 1.5, and 2.2 atm. In Fig. 16, a Mach number of 0.8 was chosen to illustrate the Reynolds number effects at subsonic test conditions. The effects shown are small but systematic. There appears to be a *Cp* increase that varies with tunnel total pressure. The most likely cause for this phenomenon is the change in test section boundary layer growth that occurs at the different Reynolds numbers. Boundary layer growth forces differing amounts of slot cross flow and consequent changes in the pressure differential between the plenum chamber and test section. Figure 17 illustrates the Reynolds number effects for Mach 1.2. The most obvious difference between the supersonic and subsonic Reynolds number effects is the pressure disturbance that appears on the static pipe 20 to 70 in. downstream of the start of the test section slots. The disturbance is believed to be caused by diffuse tunnel shocks that arise near the slot origin in response to the slight changes in slot mass flow.

3. Centerline versus 33 in. below centerline

Figure 18 shows the difference between the *Cp* distribution on the tunnel centerline and 33 in. below the centerline for Mach 0.8. These differences are minor in the regions where most wind tunnel models are positioned: TS 106 for semi-span models and TS 155 to 165 for full-span models.

C. Calibration results for flow uniformity

1. Flow angle

Flow-angularity results for Mach 0.8 and $P_{T,sc}$ = 3180 psf at TS 165 are presented in Fig. 19. For the planar survey, measurements were made over the range defined by $y = \pm 36$ in. and $z = \pm 36$ in. The vector plot shows very small flow angles especially in the core region where models are tested. Statistics for all the measurements in this plane yield an average and standard deviation of 0.08° and 0.044° for the *A*-plane flow angle and 0.04° and 0.061° for the *B*-plane flow angle. The slightly larger flow angles measured closest to the tunnel walls may be a result of the flow field being deflected by the survey apparatus itself. Premodernization flow-angle surveys measured large flow-angle gradients on the centerline within several feet of the test section floor. Values for α and β were as much as 0.35° at $z = -26.4$ in. Figure 19 clearly shows that this anomaly is no longer present in the flow. The improvement in the test section flow angularity is attributed to the addition of the honeycomb in the settling chamber.

2. Total pressure

The total pressure variation for Mach 0.85 and $P_{T,sc}$ = 2120 psf is presented using a contour plot of $C_{PT,\mathrm{cor}}$ (Fig. 20). The figure shows a small variation in the test section total pressure from that measured by the facility probes. Values for $C_{PT,\mathrm{cor}}$ are largest at the centerline and drop to zero near the test section walls. Measurements made in the test section prior to the addition of the TRS showed good agreement with those measured by the facility total pressure probes. At that time, facility total pressure was measured using probes located on the centerline, mounted off the turning vane set just upstream of the contraction. The variation in P_T shown in Fig. 20 is a result of the introduction of the TRS. Pressure losses resulting from the honeycomb and screens are a function of the dynamic pressure entering the TRS, which varies across the radius. Pressure loss across the TRS is, therefore, nonuniform and largest at the centerline.

3. Total temperature

The total temperature variation for Mach 0.85 and $P_{T,sc}$ = 2120 psf is presented in Fig. 21 using a contour plot of $\Delta T = (T_{T,\mathrm{probe}} - T_{T,F})$. The data show a slight increase in the total temperature above the centerline, but the levels measured are within 2 °F.

4. Boundary layer

Boundary layer measurements are useful for determining the proper standoff height for semi-span models. Figures 22 and 23 present the displacement thickness and momentum thickness for Mach 0.4 and 0.8 for $P_{T,sc}$ = 3180 psf from three sets of data. Data at TS 36 are for floor slots normal, which is influenced by flow exchange between the test section and the plenum. Data at TS 176 are with the floor sealed and give the upper bound for determining the proper standoff height for semi-span models. Data at TS 106 are from a premodernization test with the floor slots sealed and are within the bound defined by the data at TS 176.

IX. Conclusion

A series of calibration and flow survey tests were conducted in the 11-by 11-Foot TWT. The objective of these tests was to determine the test section static and total pressure calibration tables for the full-span and semi-span test section configurations. A static pipe was used to measure the longitudinal static pressure distribution through the nozzle and test section. A survey rake was used to measure the total pressure, total temperature and flow angle uniformity at two tunnel stations.

Results from the static pipe test identified several factors that influenced the measurements. These included effects of the slots, the effect of the mounting hardware, tap and pipe joint effects and the selection of instrumentation. In addition, variations in the static pressure with both Mach number and Reynolds and minor differences with the pipe at centerline and 33 inches below centerline were observed. The calibration tables were determined from curve-fits of the data. The flow uniformity survey showed improvements in the flow angularity and identified a small loss in total pressure due to the addition of the TRS.

A key to the success of the calibration was the use of uncertainty analysis early on to select the instrumentation thereby limiting the error in Mach number measurement to within the goal of 0.001.

References

[1] Kmak, F.J., "Modernization and Activation of the NASA Ames 11-By 11-Foot Transonic Wind Tunnel", Paper# 2000-2680, 21st AIAA Advanced Measurement and Ground Testing Technology Conference, Denver, CO, June 19-20, 2000.

[2] Kmak, F., Hudgins, M., and Hergert, D., "Revalidation of the NASA Ames 11-By 11-Foot Transonic Wind Tunnel With a Commercial Airplane Model", Paper# 2001-0454, 39th AIAA Aerospace Sciences Meeting & Exhibit, Reno, NV, January 8-11, 2001.

[3] Amaya, M.A., and Murthy, S.V., "Flow Quality Measurements in the NASA Ames Upgraded 11-By 11-Ft Transonic Wind Tunnel", Paper# 2000-2681, 21st AIAA Advanced Measurement and Ground Testing Technology Conference, Denver, CO, June 19-20, 2000.

[4] NASA Ames Research Staff, "Equations, Tables and Charts for Compressible Flow", NACA TR-1135, 1953.

Appendix

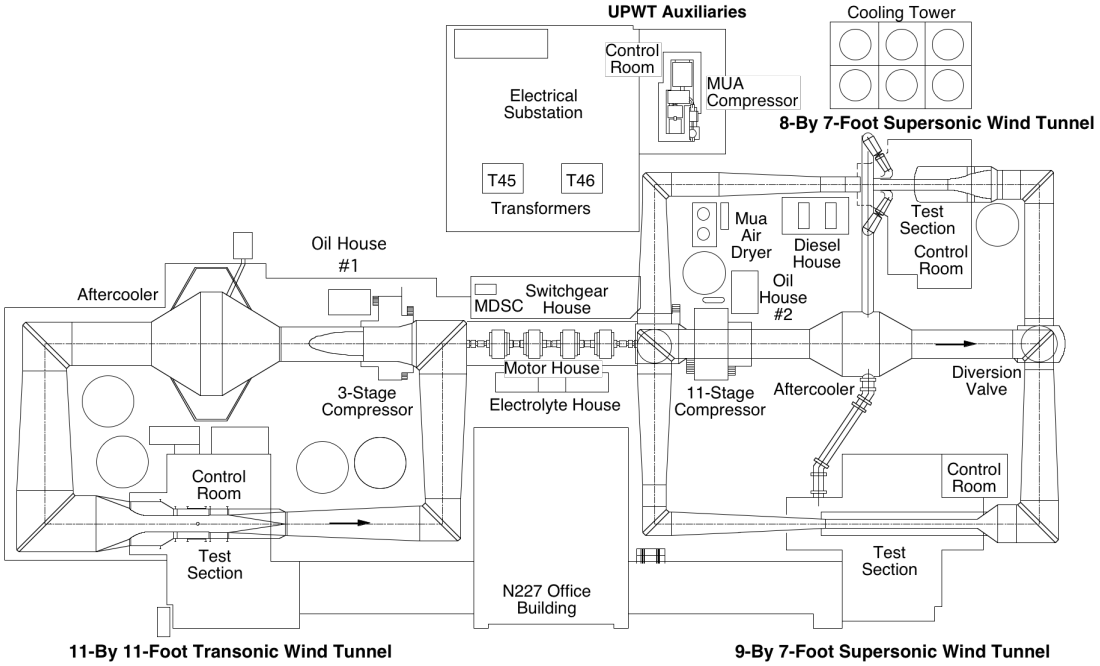

Figure 1. Unitary Plan Wind Tunnel (UPWT) At the NASA Ames Research Center.

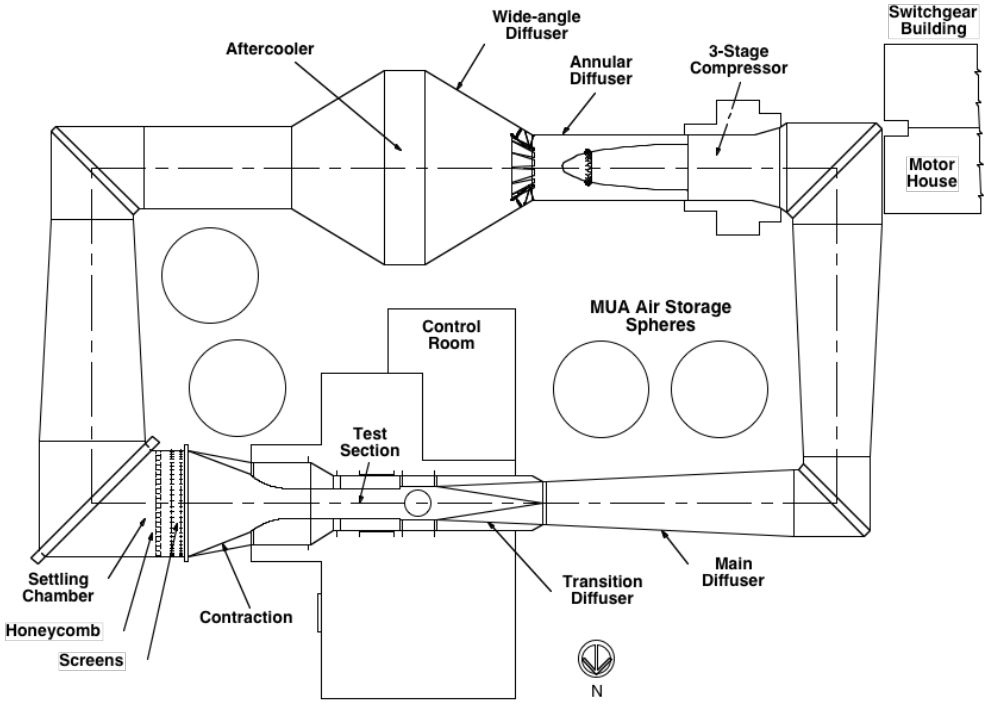

Figure 2. 11-By 11-Foot Transonic Wind Tunnel.

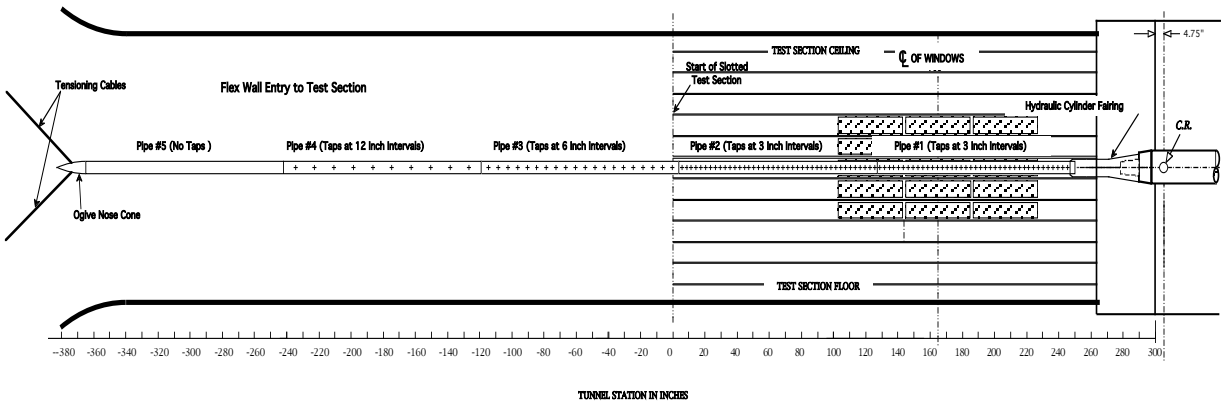

Figure 3. Static pipe installation in the 11-By 11-Foot Transonic Wind Tunnel.

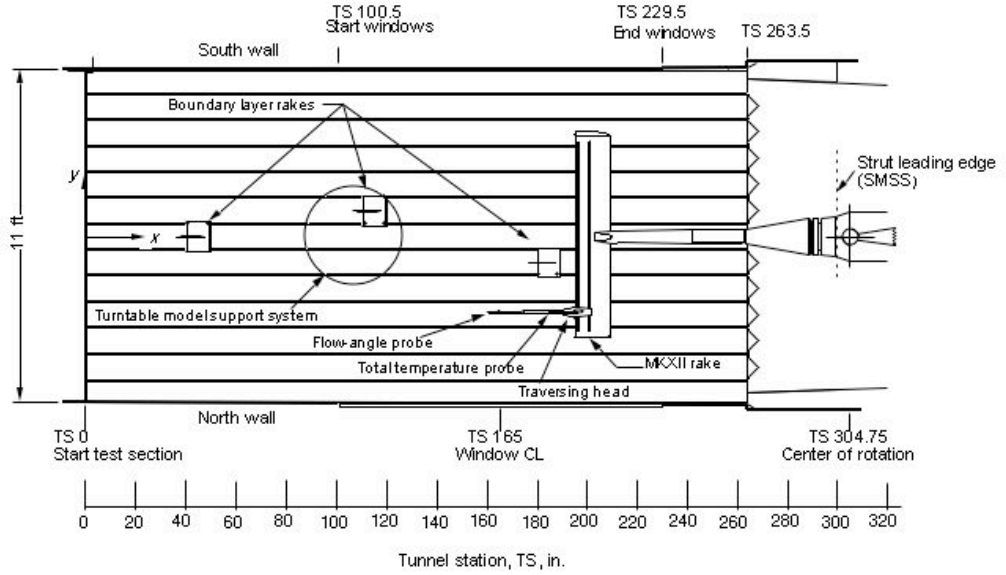

Figure 4. MK XII installation in the 11-By 11-Foot Transonic Tunnel.

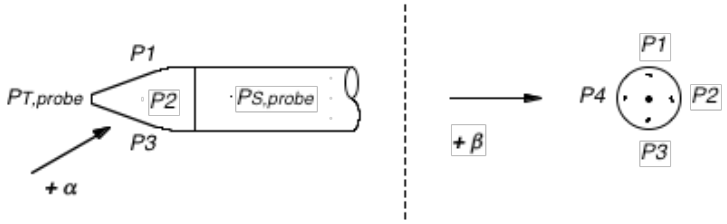

Figure 5. Five-hole cone probe.

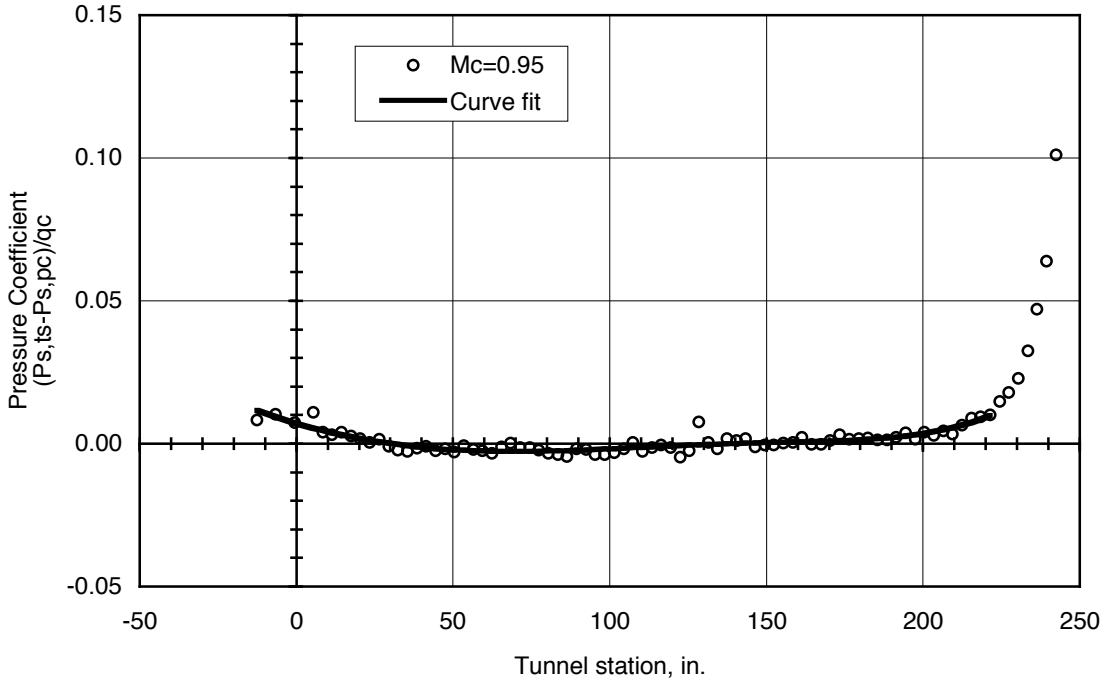

Figure 6. Average centerline *Cp* distribution and curve fit for $M = 0.95$, $P_{T,sc} = 2125$ psf; Sample duration is 1.0 second; number of data points, 120.

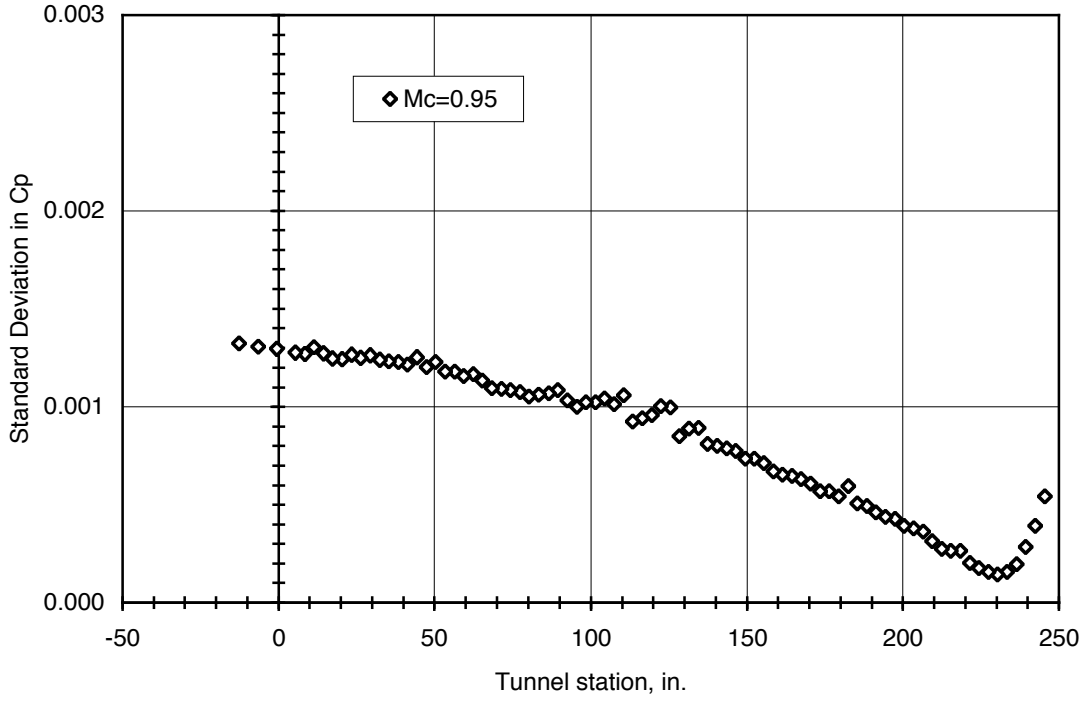

Figure 7. Standard deviation in the centerline *Cp* distribution for $M = 0.95$, $P_{T,sc} = 2125$ psf; Sample duration is 1.0 second; number of data points, 120.

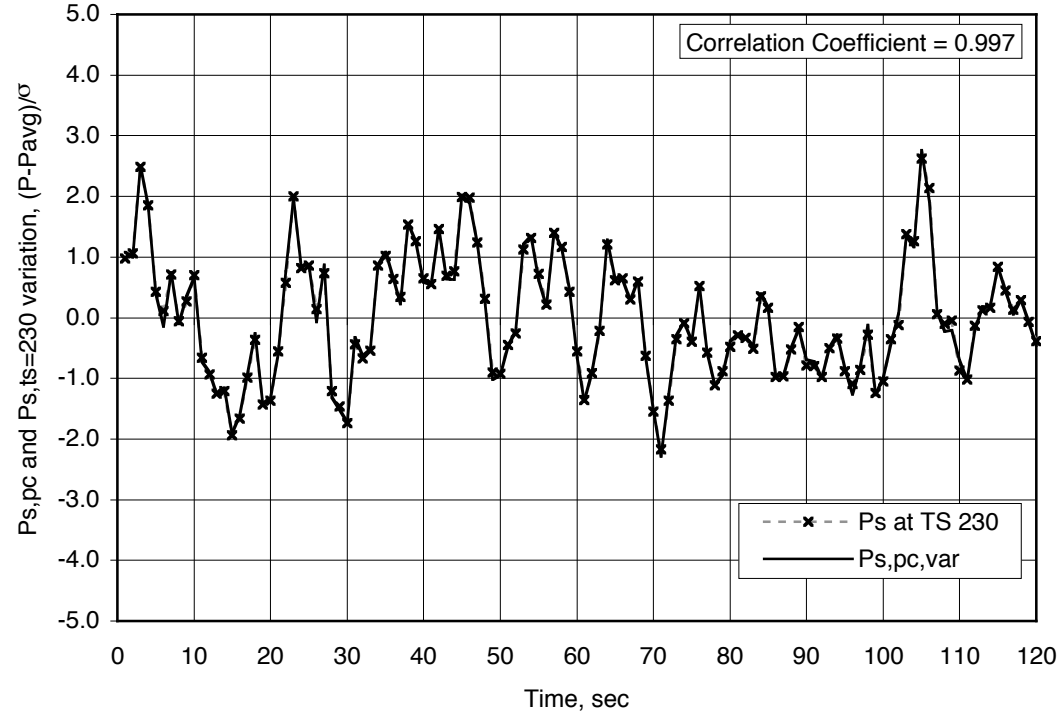

Figure 8. Temporal variation of test section pressure at tunnel station 230 for M = 0.95, $P_{T,sc}$ = 2125 psf; Sample duration, 1 sec; correlation coefficient, 0.9970; $P_{S,pc}$, 1187.7 psf; $\sigma_{Ps,pc}$, 1.29 psf; $P_{S,pipe,avg}$, 1204.97 psf; $\sigma_{PS,pipe}$, 1.22 psf.

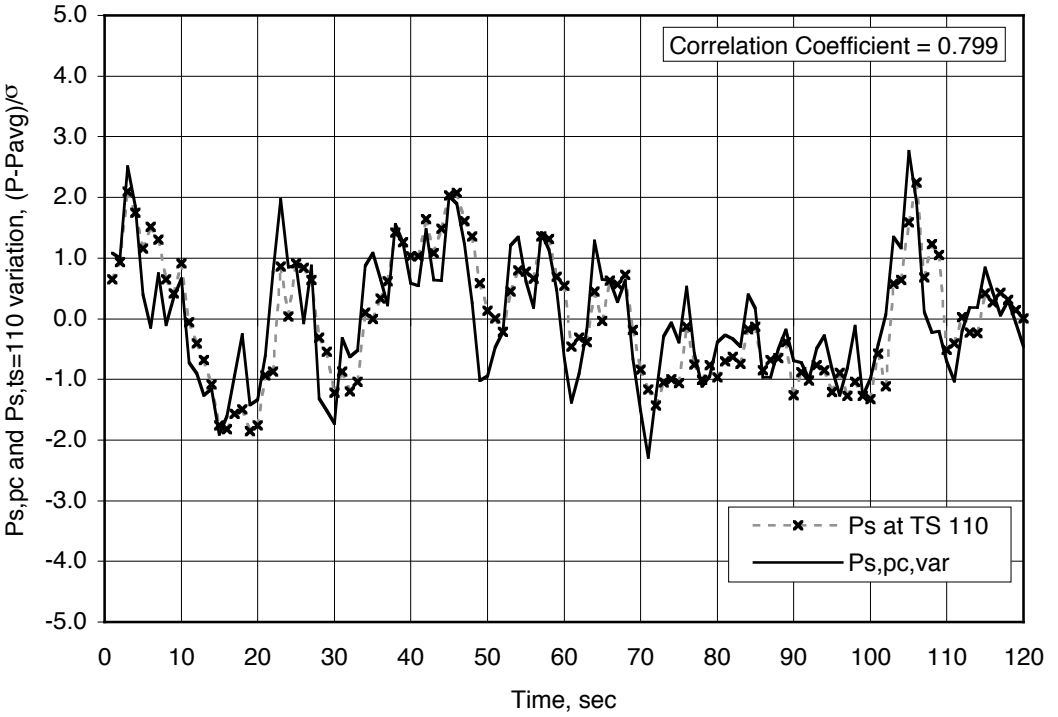

Figure 9. Temporal variation of test section pressure at tunnel station 110 for for M = 0.95, $P_{T,sc}$ = 2125 psf; Sample duration, 1 sec; correlation coefficient, 0.799; $P_{S,pc}$, 1187.7 psf; $\sigma_{PS,pc}$, 1.29 psf; $P_{S,pipe,avg}$, 1185.60 psf; $\sigma_{PS,pipe}$, 0.84 psf.

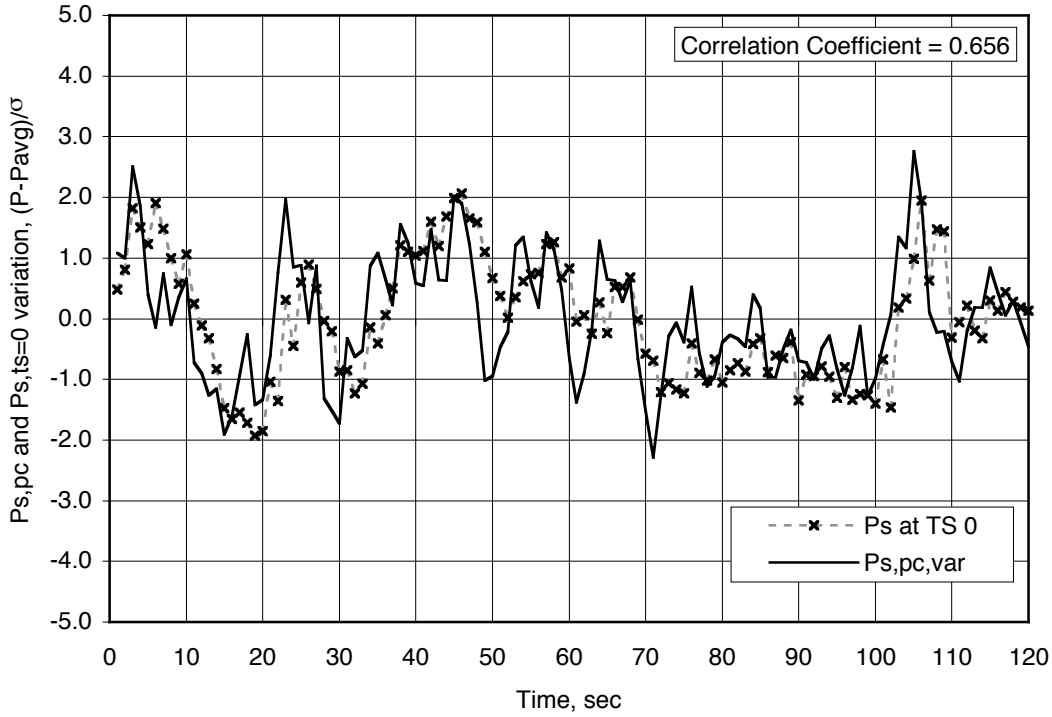

Figure 10. Temporal variation of test section pressure at tunnel station 0 for for M = 0.95, $P_{T,sc}$ = 2125 psf; Sample duration, 1 sec; correlation coefficient, 0.656; $P_{S,pc}$, 1187.7 psf; $s_{Ps,pc}$, 1.29 psf; $P_{S,pipe,avg}$, 1193.25 psf; $s_{PS,pipe}$, 0.72 psf.

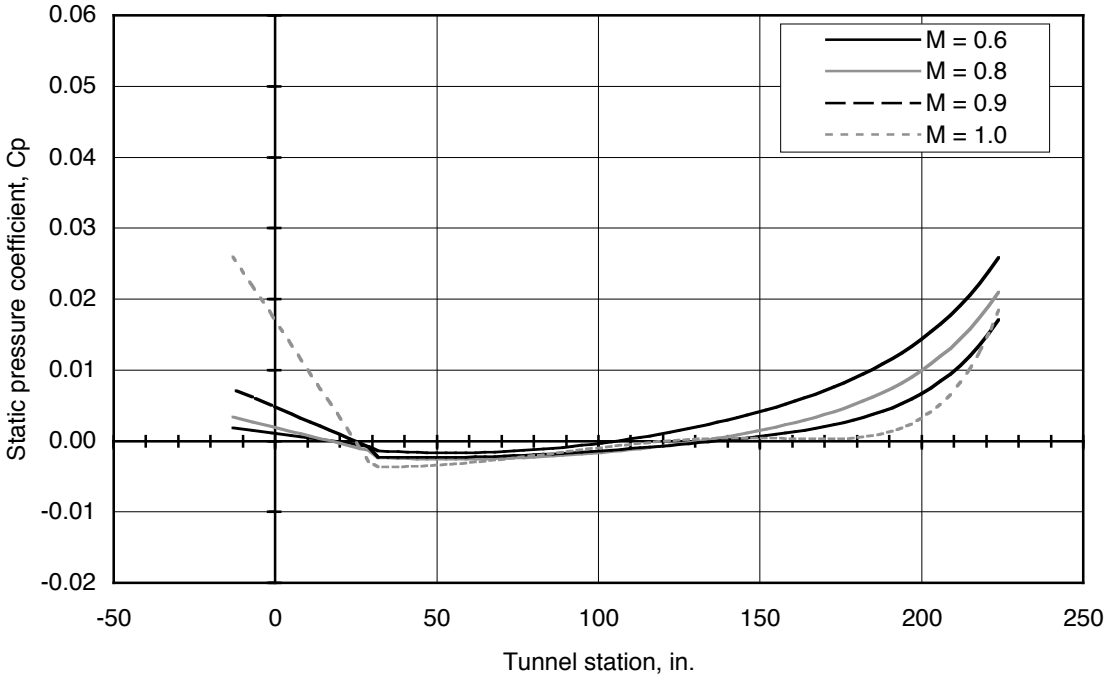

Figure 11. Effect of test section slots on centerline static pipe *Cp* distribution, $P_{T,sc}$ = 2127 psf.

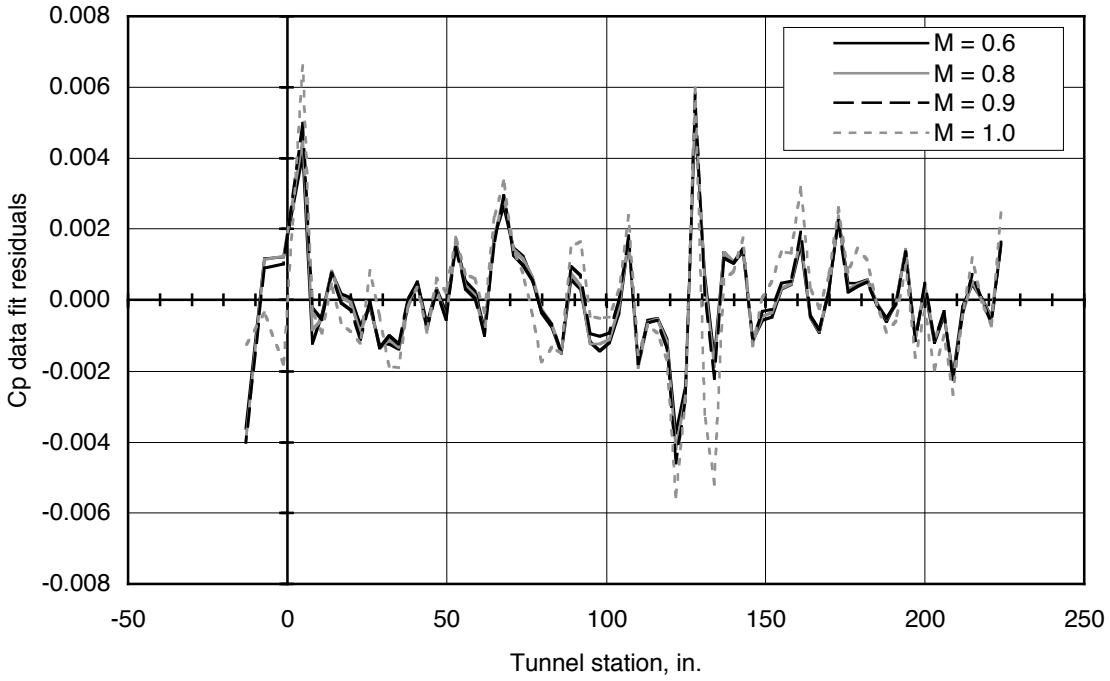

Figure 12. Tap error distribution along static pipe, $P_{T,sc}$ = 2127 psf.

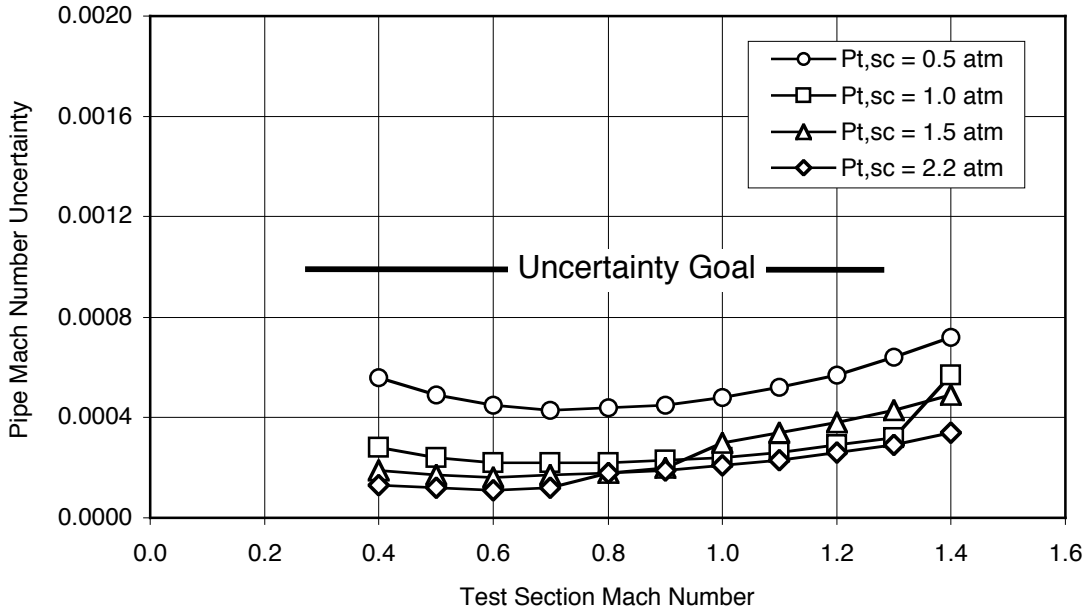

Figure 13. Uncertainty analysis predictions based on ±5 psid DTC pressure scanning modules and flow reference system.

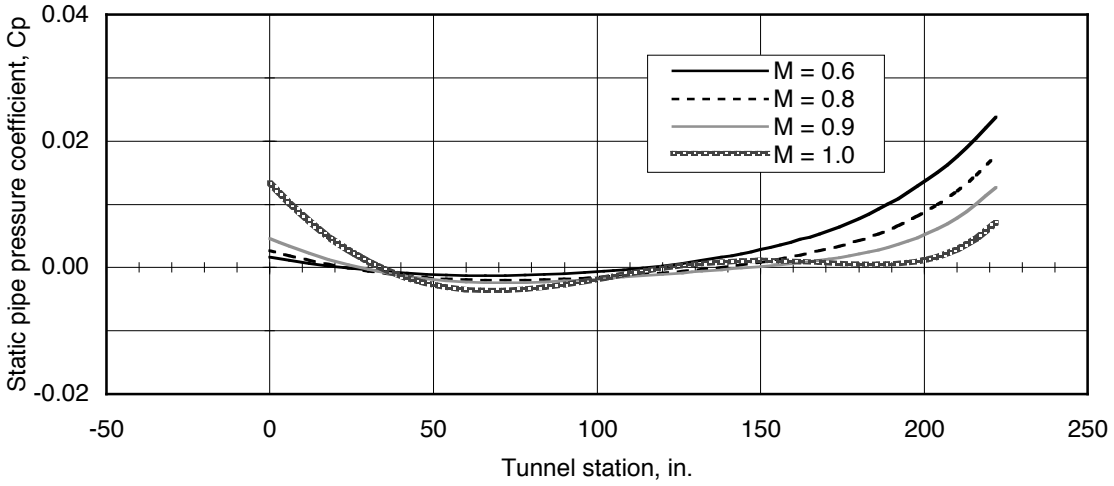

Figure 14. Subsonic Mach number effects on centerline *Cp* distribution at $P_{T,sc}$ = 2125 psf.

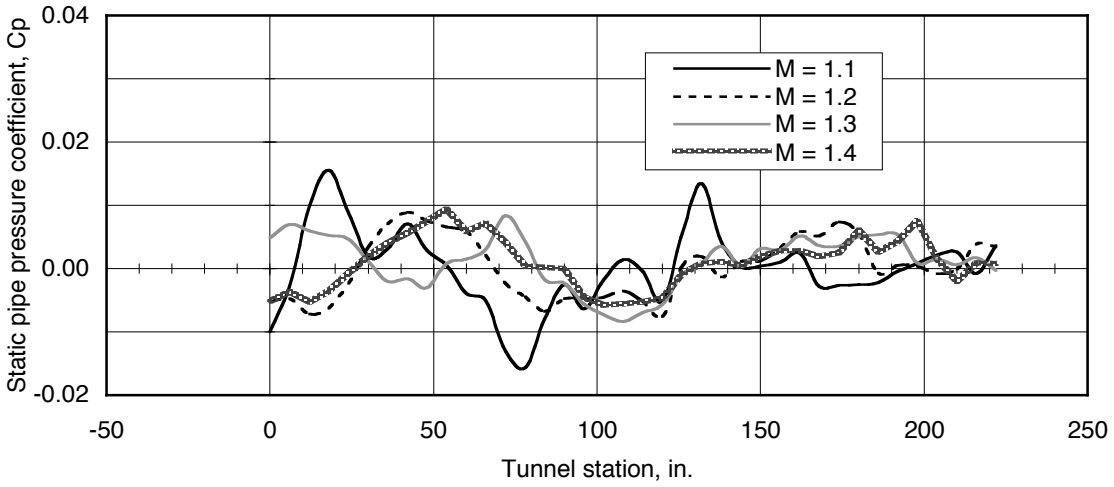

Figure 15. Supersonic Mach number effects on centerline *Cp* distribution at $P_{T,sc}$ = 2125 psf.

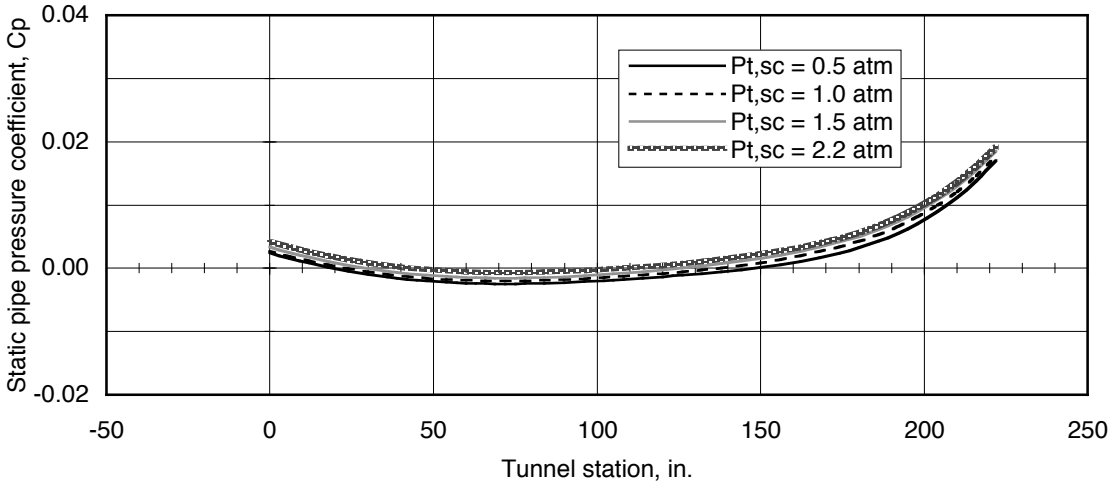

Figure 16. Reynolds number effects on centerline *Cp* distribution at *M*=0.8.

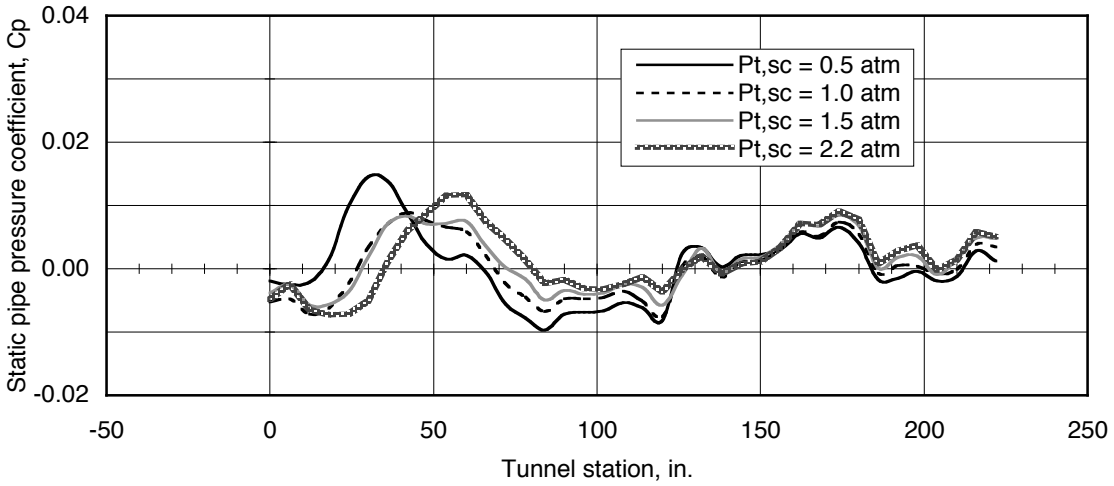

Figure 17. Reynolds number effects on centerline *Cp* distribution at *M*=1.2.

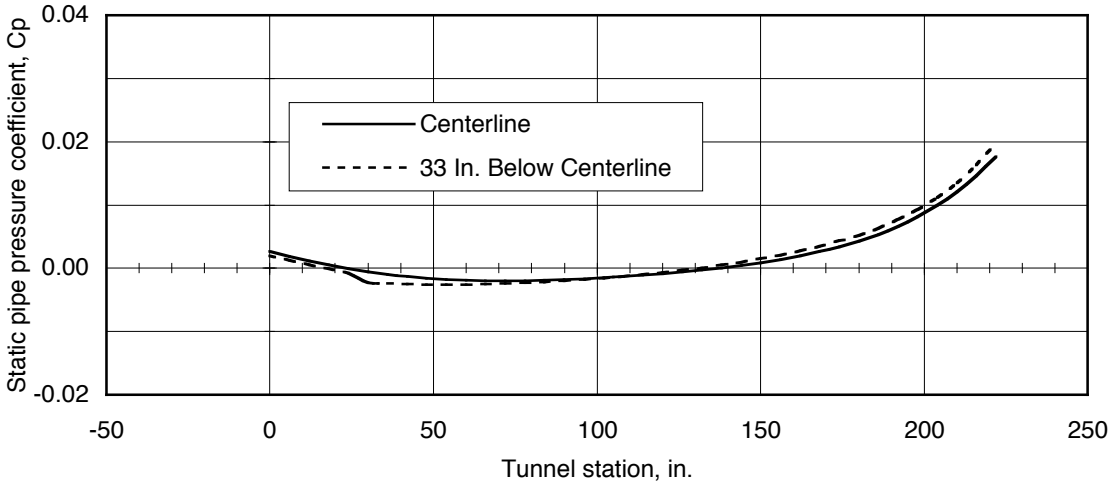

Figure 18. Effect of vertical height on centerline *Cp* distribution at $P_{T,sc}$ = 1 atm and *M* = 0.80.

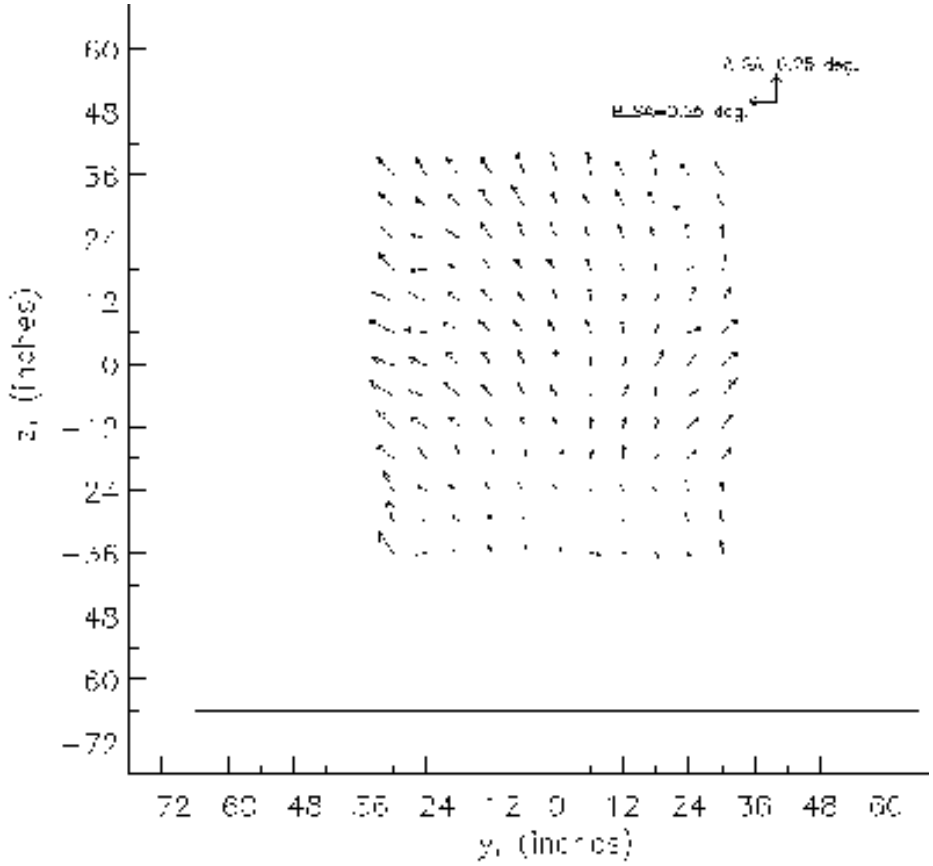

Figure 19. Flow angularity at tunnel station 160 at Mach 0.80; $P_{T,sc}$, 2119 psf; $T_{T,F}$, 80.7 °F; Average pitch angle = 0.08°; standard deviation of pitch angle = 0.044°; Average yaw angle = 0.04°; standard deviation of yaw angle = 0.061°.

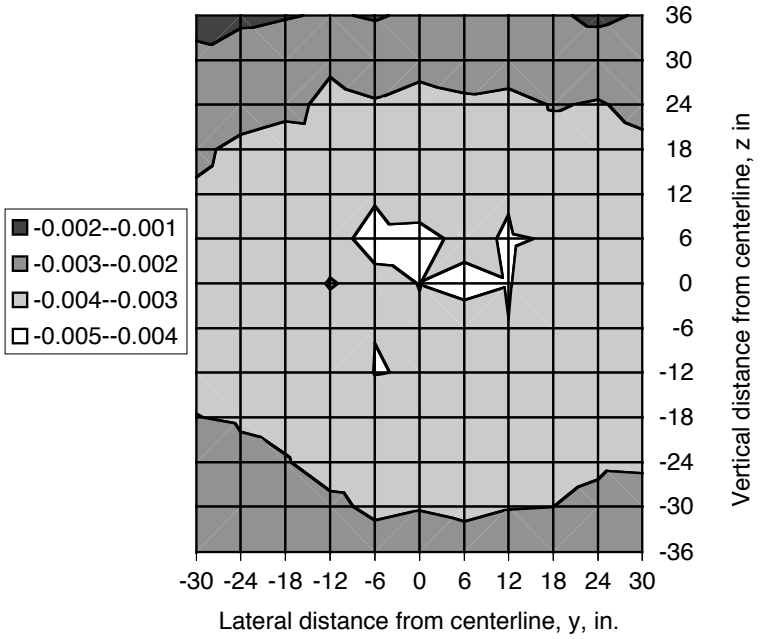

Figure 20. Total pressure correction coefficient (P_T=($P_{T,probe}$-$P_{T,sc}$)/q) contour at TS 159.5 for M = 0.85, $P_{T,sc}$ = 2120 psf.

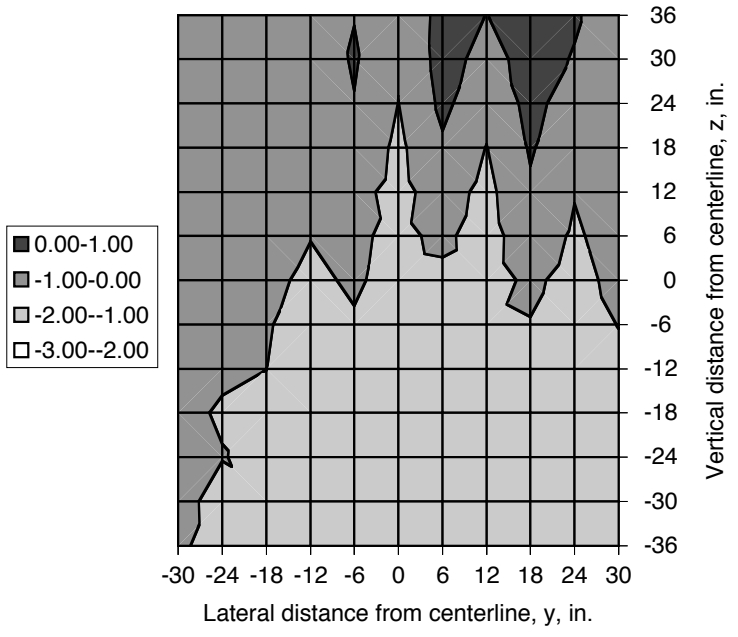

Figure 21. Total temperature contour (ΔT=$T_{T,probe}$-T_T °R) at TS 185 for M = 0.85, $P_{T,sc}$ = 2120 psf.

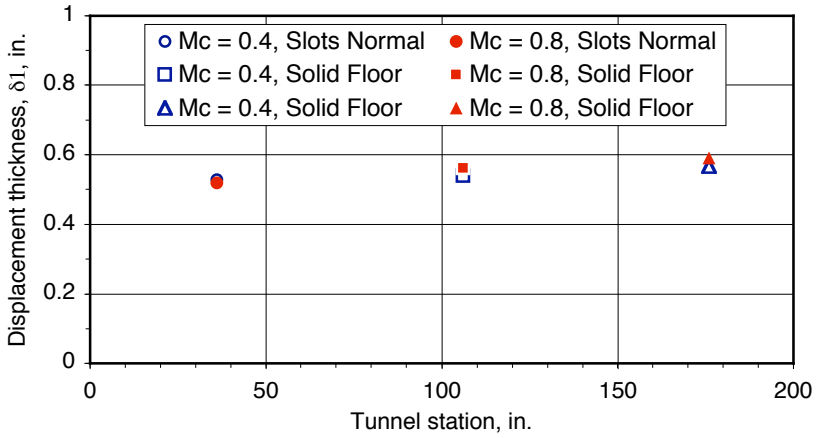

Figure 22. Boundary layer displacement thickness at M=0.4 and M=0.8 for $P_{T,sc}$ = 3180 psf.

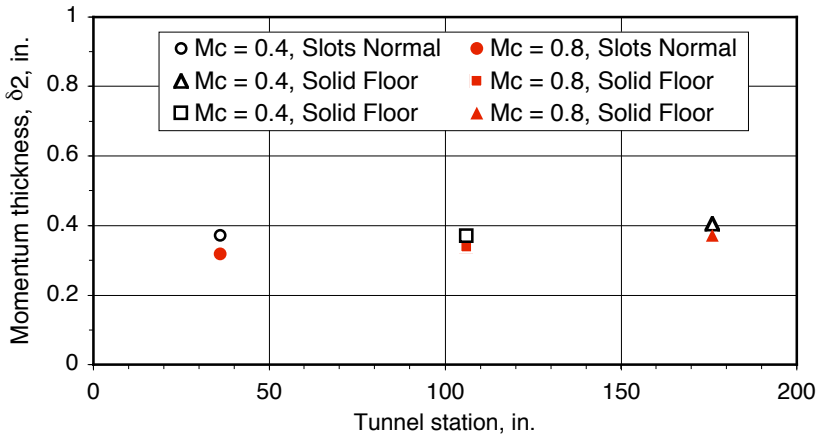

Figure 23. Boundary layer momentum thickness at M=0.4 and M=0.8 for $P_{T,sc}$ = 3180 psf.